Adv Polym Sci (2016) 270: 77–106
DOI: 10.1007/12_2015_316

Published online: 17 May 2015

Reversible Addition-Fragmentation Chain Transfer Polymerization from Surfaces

Youliang Zhao and Sébastien Perrier

Abstract Reversible addition–fragmentation chain transfer (RAFT) polymerization-based surface modification has emerged as a powerful tool for preparation of well-defined polymers grafted solid substrates. Combination of the RAFT process with highly efficient ligation reactions involving click chemistry can further extend its application in controlled synthesis of functional hybrid and composite materials. This review highlights some basic features of this method and describes synthesis of polymer-grafted solid surfaces such as silica particles, metal oxide, gold nanoparticles, cellulose, and graphene oxide. Applications of such functional materials, including their use in functional additives, bioactive surfaces and biomaterials, stationary phases for chromatographic applications, and preparation of hollow capsules and molecularly imprinted polymer films, are also summarized.

Keywords Click chemistry • Graft reaction • Hybrid material • Post-polymerization modification • RAFT polymerization • Surface modification

Contents

Y. Zhao (✉)
Suzhou Key Laboratory of Macromolecular Design and Precision Synthesis, Jiangsu Key Laboratory of Advanced Functional Polymer Design and Application, College of Chemistry, Chemical Engineering and Materials Science, Soochow University, Suzhou, 215123, China
e-mail: ylzhao@suda.edu.cn

S. Perrier
Department of Chemistry, The University of Warwick, Gibbet Hill, Coventry CV4 7AL, UK

Faculty of Pharmacy and Pharmaceutical Sciences, Monash University, 381 Royal Parade, Parkville, VIC 3052, Australia
e-mail: s.perrier@warwick.ac.uk

1 Introduction to the RAFT Process

Reversible addition–fragmentation chain transfer (RAFT) polymerization [1, 2] proceeds by a degenerative chain transfer mechanism in which a thiocarbonylthio group is exchanged between growing polymeric chains. The RAFT process was developed independently by Moad, Rizzardo, and Thang from the Commonwealth Scientific Research Organisation (CSIRO) group [3] and Zard and coworkers in collaboration with Rhodia [4]. The technique developed by Zard and coworkers, although mechanistically identical to that developed by the CSIRO group, used xanthates as the transfer agent and was coined "macromolecular design via the interchange of xanthates" (MADIX). Because these techniques only differ in the nature of the chain transfer agent (CTA), both are referred to here as RAFT for clarity.

The reactivity and, hence, suitability of a RAFT agent (CTA) for polymerizing different monomers is determined by the nature of the R and Z substituents. The Z-group influences both the activity of the thiocarbonyl group for radical addition and the stability of the resulting radical species, whereas the R-group initiates the growth of new polymeric chains. RAFT polymerization consists of the addition of a small amount of thiocarbonyl thio-based CTA to a conventional free radical polymerization system. The mechanism is thought to occur as described in Scheme 1. This mechanism comprises an initiation step (I) in which radicals are produced, for instance from thermal decomposition of a radical initiator (e.g., AIBN). These radicals then react with monomer, forming oligomers, before reacting with the RAFT agent (II). As the reactivity of the thiocarbonyl thio group is higher than that of the monomer, most of the RAFT agent is consumed to form oligomeric adducts before propagation occurs. This adduct can then fragment back to the oligomer and original RAFT agent, or form an oligomeric RAFT agent and R-group radical that can then reinitiate (III). To ensure that the

(I) Initiation

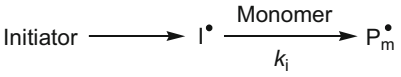

(II) Chain transfer

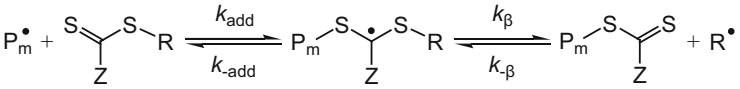

(III) Reinitiation/Propagation

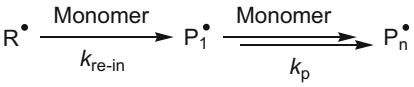

(IV) Chain equilibration

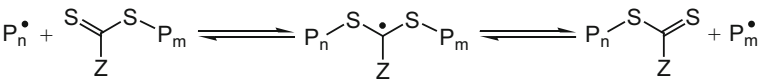

(V) Termination

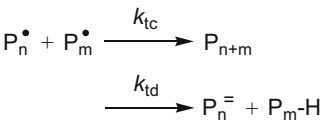

Scheme 1 Generally accepted mechanism for RAFT polymerization, showing stages *I–V*. Adapted from Perrier and Takolpuckdee [2]

reaction is controlled, the R-group must fragment from the RAFT agent at least as fast as the monomer or initiator, and reinitiate polymerization effectively. After this initial step, the reaction proceeds under equilibrated conditions, with radicals propagating and regularly transferring to the RAFT agent (IV). The kinetics of RAFT polymerization is close to that of conventional free radical polymerization, and is typically governed by the monomer concentration, with termination events determined by the amount of initiator that has decomposed. This is a feature of the RAFT process; unlike other types of living radical polymerizations, the number of dead chains in a RAFT system is exactly known because it corresponds to the number of initiating radicals (assuming no side decomposition reactions of the CTA) [5]. Therefore, optimal control in short reaction times is obtained when the ratio of CTA to initiator is kept as low as possible (typically 100), and monomer concentration is maintained around 2–3 M [6–8].

The reactivity of the RAFT agent is a crucial factor in achieving controlled polymerization [9]. In addition to the R-group, which ensures effective chain transfer and reinitiation, the Z-group must be of appropriate activity for the monomer being polymerized. The Z-group both activates the thiocarbonyl bond,

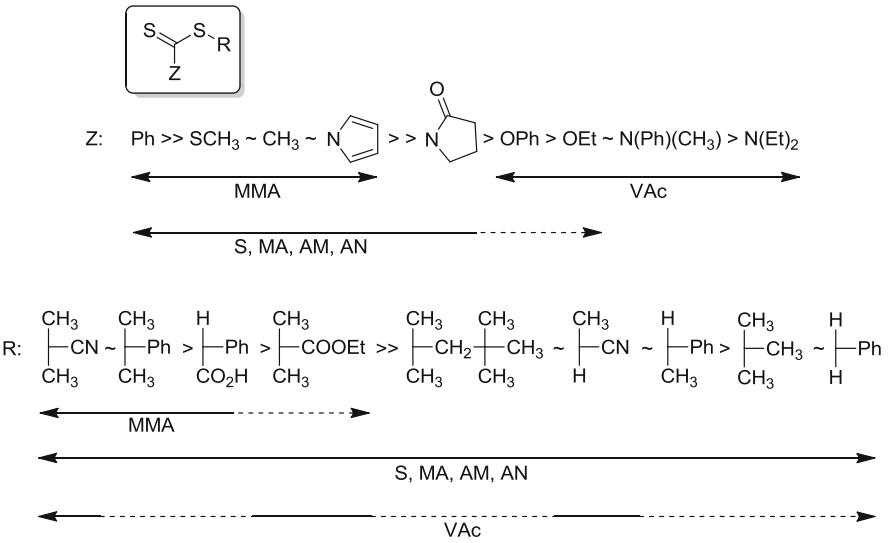

Fig. 1 Guidelines for the selection of Z-groups and R-groups for the polymerization of methyl methacrylate (*MMA*), styrene (*S*), methyl acrylate (*MA*), acrylamide (*AM*), acrylonitrile (*AN*) and vinyl acetate (*VAc*). For Z, addition rate decreases and fragmentation rate increases from *left* to *right*. For R, fragmentation rates decrease from *left* to *right*. *Dashed line* indicates partial control. Adapted from Moad et al. [9]

thus controlling the rate of addition, and stabilizes the intermediate radical, which controls the fragmentation step. The rates of addition and fragmentation required depend on the nature of the monomer being polymerized. Figure 1 shows a range of R- and Z-groups and their suitability for the polymerization of a selection of common monomers.

2 Synthetic Strategies for Surface-Grafted RAFT Polymerization

Surface-grafted RAFT polymerization differs from other techniques by the type of possible tethering points for attaching polymeric chains to the substrate surface. Grafting can occur by attaching the RAFT agent to the substrate either via its R-group (Scheme 2a) or its Z-group (Scheme 2b). Attaching the RAFT agent by its R-group is defined as a "grafting-from" approach. Using the Z-group as tethering point is often acknowledged as a "grafting-to" approach, because the chains grow away from the substrate before reacting back onto the tethered RAFT agent. Alternatively, chains can be grafted by attaching the free radical initiator to the substrate (typically a thermal initiator).

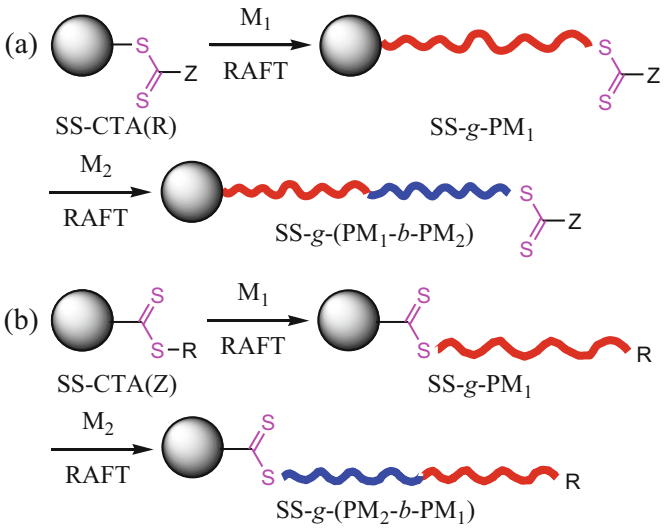

Scheme 2 Synthetic routes to diblock copolymer-grafted solid substrates (*SS*) via the R-group approach (**a**) or Z-group approach (**b**)

Tsujii et al. first described a silica-supported R-group RAFT agent prepared by transforming the bromide group of a polystyrene (PS) chain grafted onto silica by atom transfer radical polymerization (ATRP) into a dithiobenzoate. The authors then used these particles to mediate the RAFT polymerization of styrene [10]. Li and Benicewicz proposed a more direct approach to surface-initiated RAFT (SI-RAFT) polymerization by directly attaching a dithiobenzoate RAFT agent to the surface of silica particles [11, 12]. This approach is now more widely adopted, and improved control over the polymerization is obtained by introducing a free RAFT agent, which favors rapid exchange between surface-bound radicals and free chains. The free polymeric chains obtained in such a process provide a good indication of the molecular weight and polydispersity of the grafted chains [10, 13, 14]. However, at high surface density of RAFT agent, the tethered chains could have a higher molecular weight than the free chains, because slow diffusion of species leads to grafted chains growing via an uncontrolled radical process. Typically, excellent control over the polymerization is achieved, although reactions have to be kept at low monomer conversion (<20%) [14].

The ability to graft polymeric chains by tethering the RAFT agent via its Z-group is a unique feature of the RAFT process. In this approach, a propagating polymeric chain diffuses to the surface of the particle to undergo the degenerative transfer, a process closer to the grafting-to approach than the grafting-from approach. The first example of this synthetic route was provided by Perrier and Zhao, who functionalized Merrifield resin and silica particles by attaching a Z-supported RAFT agent to mediate polymerization [15–18]. The same concept

was extended to the use of xanthate, to mediate polymerization of vinyl acetate from a Wang resin [19]. A noteworthy feature of the Z-group approach is that it produces "pure" living polymeric chains, as each polymer chain bound to the particle is end-functionalized by the Z-group of the RAFT agent and can therefore be purified from dead chains, which remain in solution. This synthetic route, however, suffers from the typical drawback of the grafting-to approach: steric hindrance of the chains diffusing to the surface-anchored Z-group leads to low grafting density. Zhao et al. exploited this aspect of the reaction by reacting azide-functionalized silica particles with alkyne Z-functionalized RAFT agents in a parallel copper(I)-mediated azide–alkyne cycloaddition (CuAAC)/RAFT approach [20]. The silica–polymer core–shell nanoparticles obtained by this process were only partially grafted with polymer chains, by reaction with some azide groups. The polymer grafts were subsequently cleaved from the particles and the remaining unreacted azide groups were employed for further RAFT/CuAAC reactions. This process permits use of the silica particles as a reusable solid support to generate pure living polymers.

A very interesting study by Ranjan and Brittain compared the R- and Z-group approaches by attaching an alkyne-functionalized RAFT agent to azide-functionalized silica particles via either the R- or Z-group using CuAAC. The authors showed that a much higher grafting density could be obtained via the R-group approach than via the Z-group method [21–23]. An elegant synthesis by Rotzoll and Vana confirmed these observations: the authors grafted PMA loops to silica surfaces by employing a bifunctional RAFT agent anchored by both its R- and Z-groups [24, 25]. The polymeric chains grafted by the RAFT agent Z-group exhibited higher molecular weights than the chains obtained from an R-group-tethered RAFT agent. The authors proposed that larger propagating polymer chains were capable of reacting with the RAFT agents tethered by their Z-group as a result of the lower steric hindrance caused by low grafting densities.

In addition to Z-supported RAFT graft polymerization, some other grafting-to strategies have been developed for preparation of hybrid and composite materials. These protocols are usually based on efficient ligation reactions in which "as-prepared" RAFT polymers are attached to surface-functionalized solid substrates. Such reactions include CuAAC, thiol-based click chemistry, ligand exchange [26–29], esterification and carbodiimide chemistry [30], alkoxylsilane–hydroxyl coupling, Diels–Alder reactions [31, 32], and functional RAFT polymers as precursors or templates for formation of metal oxide nanoparticles [33, 34]. For instance, Kaupp et al. synthesized novel photosensitive RAFT agents based on *ortho*-quinodimethane (photoenol) chemistry for advanced microparticle design, in which the photoenol group reacted with dieneophiles under mild irradiation ($\lambda_{max} = 320$ nm) and ambient conditions [31]. With the aid of a light-induced grafting reaction, RAFT polymers could be grafted onto porous poly(glycidyl methacrylate) (PGMA) microspheres, and Janus microspheres could be prepared by employing a Pickering emulsion approach. Meanwhile, Kaupp et al. also reported photo-induced functionalization of spherical and planar surfaces via

caged thioaldehyde end-functionalized RAFT polymers, in which the terminal photogenerated thioaldehyde could undergo hetero Diels–Alder reactions with dienes as well as reactions with nucleophiles [32]. The terminal photoreactive polymers were photografted to porous diene-reactive polymeric microspheres to form core–shell objects with grafting densities of up to 0.10 molecules/nm^2. In addition, the versatility of the thioaldehyde ligation was evidenced by spatially resolved grafting of PS onto nucleophilic groups present in polydopamine-coated glass slides and silicon wafers via two-photon direct laser writing imaged by time-of-flight secondary ion mass spectrometry (ToF-SIMS). As an alternative to traditional polymer–metal nanoparticle hybrids prepared by ligand exchange with thiol-terminated polymers [26–29], Liu and coworkers reported an alternative approach to the size-selective and template-free synthesis of asymmetrically functionalized ultrasmall (<4 nm) gold nanoparticles (AuNPs), stably functionalized with a single amphiphilic triblock copolymer chain per nanoparticle [35]. The RAFT-synthesized copolymer had poly(ethylene oxide) (PEO) and PS outer blocks and a 1,2-dithiolane-functionalized AuNP-binding middle block, poly[lipoic acid 2-hydroxy-3-(methacryloyloxy)propyl ester-*co*-glycidyl methacrylate]. Directed nanoparticle self-assembly was used to afford organic–inorganic hybrid micelles, vesicles, rods, and large compound micelles by taking advantage of the rich microphase separation behavior of the as-synthesized AuNP hybrid amphiphilic triblock copolymers.

The use of free radical initiator tethered to a surface is an alternative approach to surface-grafted RAFT polymerization. Baum and Brittain were the first to report RAFT polymerization using a silica-functionalized free radical initiator, azoundecylchlorosilane [36]. The polymerization was mediated by a free cumyldithiobenzoate RAFT agent in solution, and yielded a mixture of free and grafted chains. Rotzoll and Vana proposed an interesting alternative method that involved attaching both a free radical initiator and a RAFT agent onto a silica particle; this strategy led to grafted particles with no observable free chains in solution [37]. More recently, Le-Masurier et al. proposed an original approach to grafting polymeric chains from silica particles coated with polydopamine [38]. The authors used a RAFT agent bearing a latent isocyanate functionality (azide carbonyl) on its R-group [39] to mediate polymerization. The carbonyl azide of the RAFT agent was converted into an isocyanate group as the R-group fragmented from the CTA, followed by rapid addition of the isocyanate onto the amine and hydroxyl groups of the polydopamine substrate. In this system, the mechanism is a hybrid between grafting-to and grafting-from in the early steps of the polymerization, but rapid addition of the isocyanate group formed in situ to the substrate ensures that the polymerization rapidly follows the traditional grafting-from route. This approach is versatile because it does not require prefunctionalization of the particles with a CTA. The approach also enables fine-tuning of the grafting density, thanks to the selectivity of the isocyanate reaction with amine (no catalyst required) and hydroxyl (catalyst required) groups.

3 Synthesis of Polymer-Grafted Solid Substrates via the RAFT Process

3.1 Polymer-Grafted Silica Particles

Silica–polymer hybrids have attracted much attention recently because of their wide range of applications in adhesion, biomaterials, coatings, composites, microelectronics, and thin films [40–45]. Thus far, silicon-based surfaces such as silica particles, silicon wafers, and polyhedral oligomeric silsesquioxanes (POSS) have been subjected to covalent modification with polymers to generate the target hybrids. Of these, silica (nano)particles have some advantages, including high mechanical strength, permeability, thermal and chemical stability, relatively low refractive index, and high surface area. They are usually chosen as ideal solid substrates for surface modification.

If polymerizable vinyl bonds are tethered to the surface of silica particles, subsequent copolymerization can be readily used to achieve silica–polymer hybrids. Guo et al. reported the synthesis of well-defined lactose-containing polymer grafted onto silica particles, in which poly(2-*O*-methacryloyloxyethoxyl-(2,3,4,6-tetra-*O*-acetyl-*β*-D-galactopyranosyl)-(1-4)-2,3,6-tri-*O*-acetyl-*β*-D-glucopyranoside) (PMAEL) obtained by cumyl dithiobenzoate (CDB)-mediated RAFT polymerization was grafted onto *γ*-methacryloxypropyltrimethoxy-modified silica particles and then deprotected to generate lactose-carrying polymer-grafted silica [46]. Chinthamanipeta et al. reported the preparation of poly(methyl methacrylate) (PMMA)–silica nanocomposites via the "grafting-through" approach, in which 3-methacryloxypropyldimethylchlorosilane was used to attach methacryl groups to the silica surface, and RAFT polymerization produced the target nanocomposites with controlled molecular weight up to 100 kDa [47]. Yang et al. synthesized silica–PS core–shell particles by SI-RAFT, in which poly(*γ*-methacryloxypropyltrimetboxysilane)-based macro-RAFT agents were immobilized onto the silica surface via a silane coupling. Subsequent grafting of polymer onto silica formed core–shell nanostructures showing a sharp contrast between silica core and polymer shell in the phase composition [48]. More recently, aerogel–PS nanocomposites with mixed free and aerogel-attached PS chains were synthesized by Sobani et al. via a grafting-through approach using 3-methacryloxypropyldimethylchlorosilane as an aerogel modifier [49].

Using Z-supported RAFT graft polymerization, Zhao and Perrier synthesized a series of homopolymer- and diblock copolymer-grafted silica particles and fumed silica. The grafted chains comprising poly(methyl acrylate) (PMA), poly(butyl acrylate) (PBA), poly(*N*,*N*-dimethylacrylamide) (PDMA), poly(*N*-isopropylacrylamide) (PNIPAM), PMMA, and PS segments usually had controlled chain length and relatively low polydispersity [16–18]. Stenzel and coworkers prepared stimuli-responsive glycopolymer brushes composed of poly(*N*-acryloyl glucosamine) (PAGA) and PNIPAM, in which the RAFT agent was immobilized on the surface of a treated silicon wafer. PAGA and PNIPAM brushes generated by

Z-supported RAFT polymerization showed a linear increase in brush thickness with the consumption of monomer in solution [50]. In addition to enhanced brush thickness after chain-extension polymerization, the suggested mechanism (whereby the second monomer NIPAM was incorporated between the first layer and the silicon surface) was further confirmed by contact angle measurements. Zhao and colleagues demonstrated that radical-induced addition–fragmentation processes between Z-supported silica and RAFT-generated polymers could be efficiently utilized for surface modification of fumed silica, and that Z-supported solid CTAs could be reused in the presence of excess sacrificial thermal initiator [51]. Nguyen and Vana performed RAFT polymerizations of styrene and MMA in bulk, mediated by fumed silica-supported CDB, in which increasing molecular weight with monomer conversion and absence of conventional polymerization activity in the interstitial solution phase were observed [52]. More recently, Vana and coworkers found that the immobilization of CTAs on silica for SI-RAFT via the Z-group approach was strongly dependent on the functionality of the RAFT-agent anchor group. Monoalkoxy-, dialkoxy-, and trialkoxy silyl ether groups were incorporated into trithiocarbonates and bound to planar silica surfaces and silica nanoparticles. It was found that the immobilization efficiency and the structure of the bound RAFT-agent film varied strongly according to the solvent used and the anchor group functionality [53]. SI-RAFT based on silica nanoparticles revealed that grafted oligomers were not formed within the crosslinked structures that originated from the immobilization. Furthermore, RAFT-agent films with less aggregation during the immobilization were more efficient during SI-RAFT in terms of polymer grafting density.

Using R-supported RAFT graft polymerization, a wide range of polymers have been grafted onto the surface of silica particles. Because this method is similar to the grafting-from approach, it allows synthesis of silica–polymer hybrids with grafting densities higher than those obtained by the Z-supported graft reaction. Benicewicz and coworkers reported the synthesis of well-defined silica nanoparticles grafted with PS, PBA, PS-*b*-PBA [11], PMMA [12], and dye-labeled poly(methacrylic acid) (PMAA) [54]. Dye-labeled PMAA-grafted nanoparticles with grafting density of up to 0.65 chains/nm^2 provided a platform to bind biomolecules and to track the movement of the nanoparticles in biological systems. On the basis of homopolymerization of styrene and alternating copolymerization of styrene and maleic anhydride (MAh), Liu and Pan prepared PS [55], P(S-*alt*-MAh), and P[S-*alt*-(MAh-*g*-PEO)] [56]. Liu et al. developed a universal route for preparation of silica-supported organic–inorganic hybrid noble metal nanomaterials, in which polymer-encapsulated gold or silver nanoparticles were synthesized and sterically stabilized by a shell layer of poly(4-vinylpyridine) (P4VP) grafted onto silica nanoparticles [57]. Using 6-(triethoxysilyl) 2-([(methylthio)carbonothioyl]thio)-2-phenylacetate, Ohno et al. synthesized monodisperse silica particles grafted with PS, PMMA, PNIPAM, and PBA [13]. As a result of the exceptionally high uniformity and perfect dispersibility, these hybrid particles could form interesting two- and three-dimensionally ordered arrays at the air–water interface and in suspension, respectively. Perrier and coworkers used the same approach to synthesize well-defined poly(4-vinylbenzyl

chloride)-grafted nanoparticles [58]. Using a grafting-from strategy, Choi et al. prepared reactive polymer brushes via surface RAFT polymerization of pentafluorophenyl acrylate, in which the reactive ester moieties were reacted with amino-spiropyrans to form reversible light-responsive polymer brush films. This was followed by a lithography technique to obtain a patterned surface of polymer brushes [59]. Conversion of the patterned polymer brushes with 5-[(2-aminoethyl) amino]naphthalene-1-sulfonic acid resulted in patterned fluorescent polymer brush films. More recently, Maleki et al. used SI-RAFT to synthesize mechanically reinforced silica aerogels with PS and PBA grafts. The aerogels exhibited a low density of 0.13–0.17 g/cm^3, high thermal insulation performance of 0.03–0.04 W/(m · K), and a high specific surface area of 350–780 m^2/g, with approximately one order of magnitude improvement in the compression strength compared with the nonreinforced aerogels [60]. It should be mentioned that hollow micro- and nanoobjects can be readily obtained if surface-grafted polymers are subjected to crosslinking and subsequent etching to remove the silica substrates. These objects have promising potential in materials science. For example, robust and narrowly distributed polymeric nanocapsules with size of 450 nm and a wall thickness of 10 nm were prepared by Huang et al. by combination of RAFT graft polymerization, photocrosslinking, and etching [61].

The combination of RAFT polymerization and highly efficient linking reaction can further extend the types of silica–polymer hybrids (Scheme 3). For instance, the coupling reaction between alkoxysilane and surface-bound hydroxyl moieties can lead not only to functional groups tethered to silica, but also to silica–polymer hybrids when alkoxysilane-functionalized polymers are used for the surface modification. Zhao and coworkers developed a combinatorial approach based on RAFT polymerization and alkoxylsilane–hydroxyl coupling to prepare silica particles grafted with well-defined homopolymers and di-, tri-, and tetrablock copolymers [62]. With *S*-methoxycarbonylphenylmethyl *S*-trimethoxysilylpropyltrithiocarbonate as RAFT agent, RAFT and chain-extension polymerization of vinyl monomers such as MA,

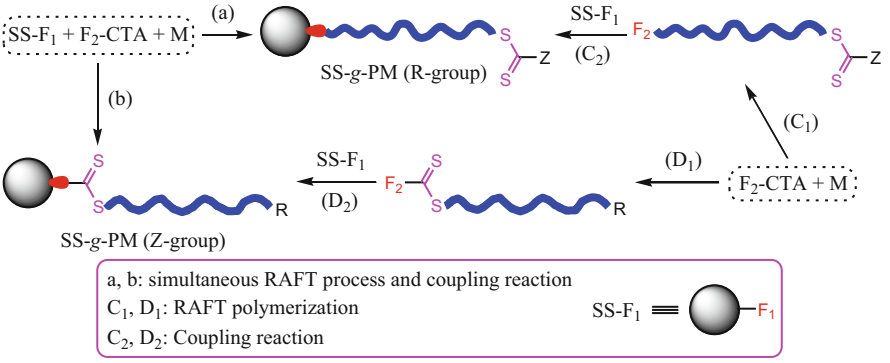

Scheme 3 Tandem (*a*, *b*) and successive (*C*, *D*) syntheses of polymer-grafted solid substrates, in which F_1–F_2 functionalities can, in theory, be any couplable moieties such as OH–$(RO)_3$Si, epoxy–COOH, azide–alkyne, and SH–en/exoxy or their precursors

BA, DMA, NIPAM, *N*-acrylomorpholine (NAM), MMA, and styrene were used to generate functional polymers, followed by a coupling reaction to synthesize the target hybrids. The grafted polymeric chains were cleaved from the surface of silica by aminolysis. Gel permeation chromatography revealed that all the grafted polymers possessed low polydispersity (typically less than 1.2) and molecular weights similar to those of the "as-prepared" polymers. Furthermore, the solid-supported polymeric chains were almost 100% living, as evident from the highly efficient chain-extension polymerization used to prepare well-defined block copolymers grafted onto silica particles. More recently, Zhao and colleagues synthesized silica nanoparticles grafted with some quaternized linear, comblike, and toothbrushlike copolymers via two-step individual reactions comprising a alkoxysilane–hydroxyl coupling reaction, quaternization, and RAFT polymerization (Scheme 4). This provides a versatile method for constructing quaternized brushes grafted onto hydroxyl-rich solid substrates [63]. Silica nanoparticles grafted with poly(*N*,*N*-dimethylaminoethyl methacrylate) (PDMAEMA) were initially prepared via tandem linking reaction and RAFT polymerization, and could act as a versatile platform for generation of three types of ion-bearing topological copolymer-grafted silica. On this basis, bromide-functionalized agents and polymers were grafted onto a surface-tethered PDMAEMA backbone to form quaternized random and comblike copolymer-grafted silica. Concurrent quaternization and RAFT polymerization were performed to generate silica nanoparticles grafted with toothbrushlike copolymers comprising PMMA, PS,

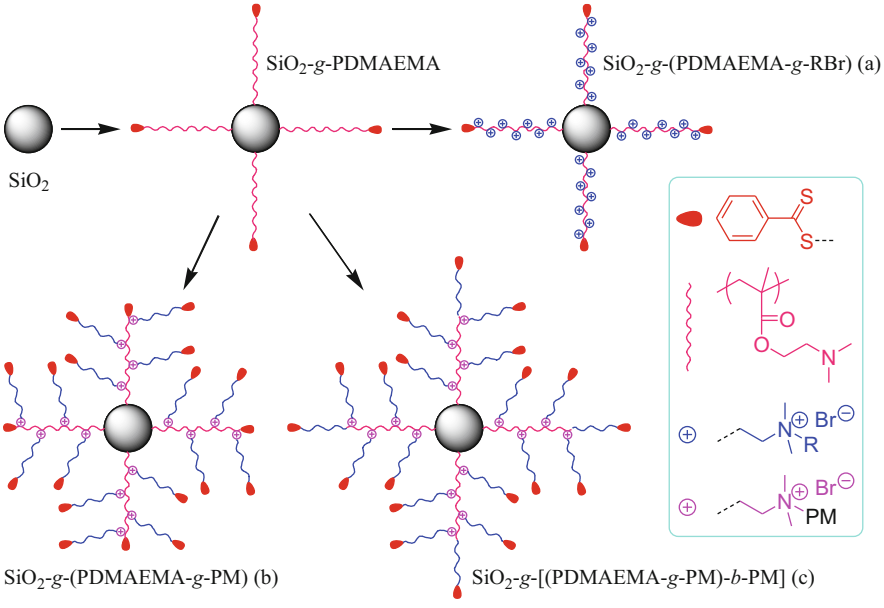

Scheme 4 Versatile synthesis of silica nanoparticles grafted with quaternized random (*a*), comblike (*b*), and toothbrushlike (*c*) copolymers via two-step reactions. Adapted from Guo et al. [63]

PNIPAM, and poly(*tert*-butyl acrylate) (P*t*BA) segments. Free polymers and grafted side chains obtained by the tandem approach usually had similar chain length and low polydispersity, and the quaternization efficiency of graft reactions was in the range 34–79% (for attaching small molecules) and 3.8–7.4% (for grafting polymeric chains). Preliminary results revealed that the surface wettability of hybrid films was dependent on factors such as macromolecular architecture, quaternization degree, chemical composition, and temperature.

An alternative approach is the use of click reactions, such as CuAAC [64–66] and thiol-based reactions [67–71], to generate silica–polymer hybrids. In their pioneering research, Ranjan and Brittain developed tandem and stepwise RAFT polymerization and click chemistry to prepare PS, PAM, and PS-*b*-PMA brushes grafted to silica nanoparticles; a wide range of grafting densities was possible [21–23]. Using the RAFT process and CuAAC, silica particles grafted with PNIPAM were prepared by Chen et al. [72]. Li and Benicewicz synthesized silica nanoparticles grafted with poly(6-azidohexyl methacrylate) and introduced various functionalities by subsequent postfunctionalization using functional alkynes via click reactions [73]. In a more recent study, Zhao and colleagues extended this method, using click chemistry to achieve highly pure block copolymers with polymeric segments such as PS, polyacrylamides, and polyacrylates [20, 74]. Tandem RAFT polymerization and CuAAC were used to prepare silica particles grafted with well-defined living block copolymers with molecular weights of up to 26,300 g/mol. Subsequent de-grafting /postmodification generated highly pure block copolymers with terminal functionalities such as thiol, methyldithio, carboxyl, hydroxyl, and halogen and also recovered surface-clickable silica particles (Scheme 5). The cycles of grafting and de-grafting reactions could be applied many times until all surface-bound clickable functionalities vanished. Kotsuchibashi

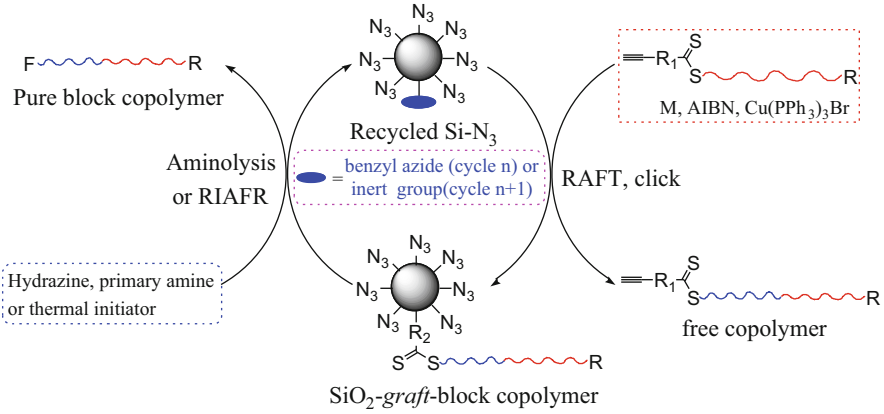

Scheme 5 Synthesis of highly pure block copolymers by combination of RAFT polymerization, azide–alkyne click reaction, and de-grafting, in which cleavage of grafted chains from a silica surface can be achieved by either aminolysis or radical-induced addition–fragmentation reactions (*RIAFR*). Adapted from Zhao et al. [20]

et al. reported preparation of temperature- and pH-responsive silica nanoparticles via simple thiol–ene click chemistry [75]. RAFT-generated PDEAEMA and PNIPAM were reduced to generate a thiol group at the chain end to react with vinyl groups on the surface of silica nanoparticles. The hybrids showed both pH- and temperature-responsive behavior and the solution properties were dependent on the ratio of the two polymers on the surface. Chen et al. reported grafting of poly (lauryl acrylate) onto nanosilica via a thiol–ene reaction, in which the trithioester terminal group of the RAFT polymer was converted to thiol and grafted onto nanosilica modified with 3-(methacryloxy)propyl-trimethoxysilane. The hybrid material has potential application in coatings or composites [76]. Peng et al. reported a facile method for combining the sol–gel reaction, RAFT process, and thiol–ene click reaction to prepare monodisperse silica–poly(*N*-vinylimidazole) core–shell microspheres of 200 nm average diameter [77]. Han et al. reported preparation of surfaces that were dual-switchable between hydrophobic and superhydrophobic by combination of RAFT and thiol–NCO chemistry, in which poly(7-[6-(acryloyloxy)hexyloxy]coumarin)-*b*-PNIPAM was grafted onto the surface of SiO_2 modified by toluene diisocyanate [78]. The static contact angle of the surface of hybrid film switched from 98° to 137° by adjusting the temperature, the contact angle also oscillated between 137° and 157° upon UV irradiation at 365 and 254 nm, respectively, revealing dual-switchable surface wettability.

3.2 *Polymer-Grafted Metal Oxide*

As a result of the strong tendency of nanoparticles such as metal oxides to agglomerate, homogeneous dispersion of these materials in a polymeric matrix is extremely important. Surfaces modified via the RAFT process have been efficiently used to prepare functional hybrids or composites, in order to avoid aggregation of nanoparticles and to enhance the filler–polymer interaction. This approach has been applied to a range of metal oxides, and examples are detailed below.

TiO_2 Hojjati et al. reported synthesis of TiO_2–PAA nanocomposites by RAFT polymerization using a bifunctional RAFT agent, 2-(butylsulfanylcarbonothioylsulfanyl) propanoic acid, with an available carboxyl group to anchor onto TiO_2 nanoparticles. Subsequent RAFT polymerization of acrylic acid (AA) formed the desired nanocomposites [79]. Ngo et al. synthesized hybrid TiO_2 nanoparticles with well-defined PMMA and poly(*tert*-butyldimethylsilyl methacrylate), in which the surface of titania nanoparticles was first modified by a coupling agent, 3-(trimethoxysilyl)propyl methacrylate (MPS), to form polymerizable particles. Then, the immobilized vinyl bond on the surface was subjected to radical polymerization in the presence of RAFT agent 2-cyanoprop-2-yl dithiobenzoate to form nanocomposites [80]. Hojjati and Charpentier reported synthesis of TiO_2–PMMA nanocomposites in supercritical CO_2 via RAFT polymerization, in which 4-cyano-4-(dodecylsulfanylthiocarbonylsulfanyl)pentanoic acid was first coordinated to the TiO_2 surface. A subsequent

RAFT process formed the target nanocomposites [81]. Crippa et al. reported preparation of high dielectric constant rutile–PS composite with an enhanced percolative threshold, in which hydrothermally synthesized TiO_2 nanocrystals were coated with PS grown by RAFT polymerization and then dispersed into a PS matrix at various concentrations [82]. It was found that the polymer molecules attached to the surfaces of nanoparticles existed in a brush regime, and that the rutile nanoparticles self-assembled into chestnut-burr aggregates whose number increased with increasing filler amount. With increasing filler concentration, the composites displayed a higher dielectric constant as a result of the self-assembly of rutile nanoparticles into chestnut-burr aggregates, where rutile crystals could share lateral faces and form capacitive microstructures.

Quantum Dots The polymeric functionalization of quantum dots (QDs) via ligand exchange is a robust method for the preparation of stable fluorescent particles with high quantum yields. For most biological applications of QDs, water solubility is a key requirement. To achieve biocompatibility, polymeric ligand systems that can provide water solubility as well as effective anchoring groups are advantageous. Viswanath et al. prepared multiply binding histamine ligands for the robust functionalization of QDs, in which histamine functional polymers bearing poly (ethylene glycol) (PEG) side chains were coated onto the surface of oleate-capped CdSe/$Cd_xZn_{1-x}S$ QDs via ligand exchange [83]. Esteves et al. reported synthesis of QD–polymer nanocomposites by RAFT polymerization in miniemulsion using a grafting-from approach, in which the surfaces of CdS and CdSe QDs were modified by PS and PS-*b*-PBA grafts [84]. Liu et al. presented some polymeric ligands for QD water solubilization to yield biocompatible and derivatizable QDs with compact size, high quantum yields (>50%), excellent stability across a large pH range (pH 5–10.5), and low nonspecific binding [85]. Das and Claverie developed a simple route for the preparation of PbS QDs embedded into polymeric nanospheres by emulsion polymerization, in which QDs were first dispersed in an aqueous solution containing a statistical oligomer with butyl acrylate and acrylic acid units, and then an emulsion polymerization process was performed to obtain core–shell nanoparticles [86]. Dilag et al. reported controlled fabrication of CdS/PDMA, CdS/poly(DMA-*co*-MMA), and CdS/poly(DMA-*co*-styrene) fluorescent QD nanocomposites for use as latent fingermark developing agents on nonporous surfaces [87]. The intrinsic optical properties of CdS QDs were retained throughout the synthetic pathways, which allowed for the successful one-step application and fluorescent visualization of latent fingermarks (fresh and aged) on aluminum foil and glass substrates under UV illumination.

Magnetic Nanoparticles Boyer et al. prepared antifouling magnetic nanoparticles (MNPs) for siRNA delivery by coating iron oxide nanoparticles (diameter of 8 nm) with poly[oligo(ethylene glycol) methyl ether acrylate] and poly(dimethylaminoethyl acrylate) (PDMAEA) [88]. Li et al. reported shape-controlled synthesis of glycopolymer-coated iron oxide nanoparticles, in which RAFT-synthesized glycopolymers were conjugated to spindle and cube-like iron oxide nanoparticles coated with dopamine methacrylamide. The resultant glyco-nanoparticles with

variable shapes had shape-dependent cell uptake behavior and enhanced activity towards specific lectins [89]. Sahoo et al. prepared thermo- and pH-responsive polymer-tethered multifunctional MNPs for targeted delivery of anticancer drugs [90]. MNPs were first surface-modified by introducing amine groups using 3-aminopropyl-triethoxysilane; then, RAFT-synthesized dual-responsive PNIPAM-*b*-PAA was attached to the amine-functionalized MNPs via the EDC/NHS method. Folic acid was tethered to the surface to accomplish cancer-specific targeting properties, and rhodamine B isothiocyanate was conjugated to endow the MNPs with fluorescence for cellular imaging applications. These nanoparticles were capable of target-specific release of loaded anticancer drug doxorubicin in response to pH and temperature and, hence, could serve as potential drug carriers for in vivo applications. More recently, Wang et al. reported a new combination of recyclable MNPs, polymers, and antibiotics that showed increased effectiveness in combating bacterial infections [91]. The strategy of direct co-precipitation of iron salts was used to generate superparamagnetic nanoparticles with a saturation magnetization of 59.5 emu/g. A silica coating was applied and used to stabilize the MNPs and create a convenient platform for further functionalization, followed by SI-RAFT to graft a variety of PMAA brushes of different lengths and at different densities. The polymer-grafted MNPs were removed from aqueous solution after antimicrobial testing using a magnet to avoid nano-based pollution of the environment. The bioactivity of an antibiotic (penicillin-G) against bacteria (*Staphylococcus aureus* and *Escherichia coli*) was significantly enhanced when physically bound to the PMAA-grafted MNPs. The inhibition activity of the penicillin–nanoparticle complex was retained using recycled MNPs that had been reloaded with penicillin-G.

3.3 Polymer-Grafted Gold Nanoparticles

The grafting of polymers onto AuNPs has attracted much attention because of the multiple applications of the resulting materials, in applications ranging from materials to medicine and biology. Sumerlin et al. reported modification of gold surfaces with water-soluble (co)polymers prepared via aqueous RAFT polymerization, which enabled the immobilization of poly(sodium 4-styrenesulfonate), poly[(4-vinylbenzyl) trimethylammonium chloride], PDMA, and poly(3-[2-(*N*-methylacrylamido)ethyldimethyl ammonio]propane sulfonate-*b*-*N*,*N*-dimethylacrylamide) onto gold films [92]. Rossner and Vana reported ordered planet–satellite nanostructures using RAFT star polymers. Preparation was based on star polymers decorated with surface-tethered trithiocarbonate groups and thus provided the polymer with the ability to connect larger AuNP planets to smaller AuNP satellites [93]. This strategy offers a straightforward way to prepare AuNP scaffolds with multiple reactive functionalities at defined distances from the central core. Glycopolymer-coated AuNPs can be used as anticancer agents [94–96] and for biomolecular recognition [97]. Kirkland-York et al. reported tailored design of

AuNP-siRNA carriers utilizing RAFT polymers [98]. Duong et al. extended the application of functional AuNPs to storage and controlled release of nitric oxide using poly[oligo(ethylene glycol) methyl ether methacrylate]-*b*-poly(vinyl benzyl chloride) as precursor [99]. Thus far, a series of functional polymers have been coated on the surface of AuNPs or acted as scaffolds to stabilize AuNPs, and these polymers primarily comprise glycopolymers [100–102], PEG-bearing poly(meth) acrylates [103–105], PS [106], poly(4-vinylpyridine) (P4VP) [107], PNIPAM [108–110], poly(*N*-vinyl caprolactam) [111, 112], poly[(3-acrylamidopropyl) trimethyl ammonium chloride [113], poly(pentafluorophenyl methacrylate) [114], PDMAEMA [115, 116], and branched poly[(*S*-4-vinylbenzyl *S*′-propyl-trithiocarbonate)-*co*-PEGMA] [117].

3.4 Polymer-Grafted Cellulose

Cellulose is a highly interesting material as a result of its materials properties, abundance, renewability and low cost. The heterogeneous grafting of cellulose fibers through controlled radical polymerization methods allows preparation of fibers with tailorable properties and built-in functionalities that can act as promising materials for advanced applications [118–121].

Carlsson revealed that modification of cellulose surfaces by cationic polymer latexes could be accomplished by RAFT-mediated surfactant-free emulsion polymerization [122]. Using radiation-induced RAFT polymerization, PS [123] and PGMA [124] were grafted onto cellulose substrates. Poly(isobornyl acrylate) was grafted onto a solid cellulose substrate by combination of RAFT polymerization and hetero Diels–Alder cycloaddition [125]. Demirci et al. performed surface modification of electrospun cellulose acetate nanofibers via RAFT polymerization and found that surface-tethered poly[(4-vinylbenzyl)trimethylammonium chloride] (PVBTAC) brushes were suitable membrane materials for filtration, purification, and/or separation of DNA [126]. Perrier and coworkers synthesized PDMAEMA-grafted cellulose and showed that its antibacterial activity was dependent on the alkyl chain length and on the degree of quaternization of graft polymers [127–129]. The PDMAEMA-grafted cellulose fiber with the highest degree of quaternization and quaternized with the shortest alkyl chains was found to exhibit particularly high activity against *E. coli*. A tailor-made conjunct of methyl cellulose and poly(vinyl acetate) (PVAc) was synthesized through the combination of RAFT polymerization and a thiol–ene click reaction [130]. Yuan et al. prepared zwitterionic polysulfobetaine brushes grafted to cellulose membranes (CMs) to improve hemocompatibility and antibiofouling properties [131]. The composites had excellent hemocompatibility, featuring lower platelet adhesion and protein adsorption properties without causing hemolysis. *E. coli* and HeLa cell adhesion tests showed that grafted CMs had superior antibacterial adhesion properties and long-term cell adhesion resistance for up to 4 days, revealing their great potential for use in biomedical applications. In addition, other homopolymers and block copolymers

such as PS [132], poly(sodium 4-styrenesulfonate) [133], PMA [134], poly(2,2,2-trifluoroethyl methacrylate) [135], poly(*N*-acryloyl-L-amino acid) [136], poly (hydroxyethyl methacrylate) (PHEMA) [137], PAM [138], poly(*N*,*N*-diethyl-acrylamide) [139], PNIPAM, PAA, and their copolymers [140] were also covalently grafted onto the surface of cellulose.

3.5 Polymer-Grafted Graphene and Graphene Oxide

Graphene nanosheets possess a range of extraordinary physical and electrical properties and have enormous potential for applications in microelectronics, photonic devices, and nanocomposite materials [141–145]. However, single graphene platelets tend to undergo agglomeration as a result of strong π–π and van der Waals interactions, which significantly compromises the final material properties. One of the strategies to overcome this problem and increase graphene compatibility with a receiving polymer host matrix is to modify graphene or graphene oxide (GO) with polymer brushes. Research to date can be grouped into approaches involving grafting-from and grafting-to techniques, and into approaches relying on covalent or noncovalent attachment of polymer chains to the suitably modified graphene or GO [146–148].

Li et al. reported a GO-based molecularly imprinted polymer (MIP) platform for detecting endocrine-disrupting chemicals. The GO–MIP hybrids showed outstanding affinity towards 2,4-dichlorophenol in aqueous solution [149]. Layek et al. synthesized amphiphilic poly(*N*-vinyl pyrrolidone)-grafted graphene by RAFT polymerization for the reinforcement of PVAc films [150]. Ye et al. developed versatile grafting approaches for functionalizing individually dispersed graphene nanosheets using RAFT polymerization and CuAAC [151]. Various types of polymer chains have been covalently tethered to graphene nanosheets using these two approaches, producing various molecular brushes with multifunctional arms, resulting in water-soluble, oil-soluble, acidic, basic, polar, apolar, and variously functionalized polymers. Peeters et al. reported thermal detection of histamine with a GO-based MIP platform prepared by RAFT polymerization [152], in which MIP–GO hybrids were able to measure histamine in buffer solutions by thermal detection. Using methacrylic acid as a hydrophilic monomer, Liu et al. synthesized hydrophilic surface ion-imprinted polymers based on GO for removal of strontium from aqueous solution [153]. Thus far, a wide range of polymers such as PS [154–156], PDMAEA, PAA [157, 158], PMMA, P*t*BA and PNIPAM [159], poly[*N*-(2-hydroxypropyl) methacrylamide] [160], poly(*N*-vinylcarbazole) [161, 162] and their copolymers have been efficiently grafted onto the surface of GO and reduced GO.

In addition to SI-RAFT and click chemistry, other linking reactions such as alkoxysilane–hydroxyl coupling reactions and carboxyl–epoxy ring-opening reactions can also be efficiently used to generate well-defined polymer-grafted graphene and GO. Zhao and coworkers reported synthesis of V-shaped copolymers grafted to

GO via a combinatorial approach [163]. Starting from a monomethoxy poly(ethylene glycol) (MPEG)-based macro chain transfer agent, three kinds of triblock copolymers with epoxy, carboxyl, or methoxysilane functionalities in the central short block were synthesized via RAFT processes. Subsequent carboxyl–epoxy and hydroxyl–methoxysilane coupling reactions were used to synthesize the target V-shaped copolymer–GO nanocomposites (Scheme 6). Owing to satisfactory control over molecular weight and polydispersity of the RAFT process, the resulting triblock copolymer MPEG-*b*-PM_1'-*b*-PM_2 possessed predetermined molecular weight, low polydispersity (1.04–1.19) and precise chemical structure; PM_1' represents poly[3-(trimethoxysilyl)propyl methacrylate] (PMPS), PGMA, or PAA obtained by hydrolysis of P*t*BA; PM_2 represents PPEGMA ($M_n = 300$), PS, PNIPAM, PDMA, or PMA. By assuming that GO nanosheets have the same specific surface area as graphene (about 2,630 m^2/g), the grafting density of V-shaped grafted copolymer on each side of GO was estimated to be within 0.025–0.162 chains/nm^2. With the aid of ultrasonic treatment, V-shaped copolymer-grafted GO could be efficiently dispersed in a wide range of solvents involving hexane and toluene. The film wettability and surface morphology of GO–copolymer nanocomposites obtained were tunable by control over factors such as temperature, solvent, and amphiphilicity of grafted chains, allowing potential applications in biomaterials, nanoscience, and nanotechnology. Meanwhile, Zhao and colleagues also synthesized homopolymer- and diblock copolymer-grafted GO by simultaneous coupling reaction and RAFT process, in which a series of polymers were covalently grafted onto GO surfaces via either grafting-to or grafting-from approaches using Z-functionalized *S*-methoxycarbonylphenylmethyl *S*′-3-(trimethoxysilyl)propyltrithiocarbonate (MPTT) and R-functionalized *S*-4-(trimethoxysilyl)benzyl *S*′-propyltrithiocarbonate (TBPT) as functional RAFT

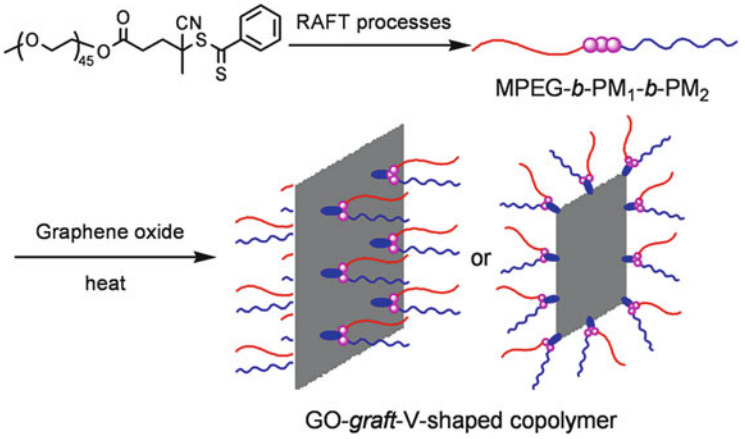

Scheme 6 Versatile syntheses of V-shaped copolymer-grafted GO. *Spherical symbols* denote monomer units with epoxy, carboxyl, or methoxysilane functionalities. Adapted from Zhang et al. [163]

agents [164]. The improved solubility and dispersibility of GO–polymer composites in various solvents, including hexane and water, confirmed their amphiphilicity. Surface morphologies involving nanosheets, nanoparticles, and nanorods were observed as the composites were dispersed in different solvents with the aid of sonication treatment, demonstrating that the grafting process can offer the opportunity to alter GO morphology.

4 Applications of Polymer-Grafted Solid Substrates

4.1 Additives to Improve Physicochemical Properties

Although silica–polymer composites can be prepared by mixing organic and inorganic components, it is difficult to obtain a homogeneous mixture [165]. To improve the compatibility between silica and polymer matrix, a popular method is to modify the silica surface using coupling agents, which not only improve the compatibility between organic and inorganic phases but also enhance the interaction between the components at the interface level. An alternative approach uses high energy plasma lasers, whereby the energetic ions from the plasma laser break the Si–C and Si–O bonds in the silane surface groups and create active sites that can react with the surrounding polymer matrix [166]. Incorporation of silica nanoparticles in the polymeric matrices gives hybrid polymer films with increased tensile strength and impact resistance, without decreasing the flexural properties of the polymer matrix. In addition to combining the flexibility and easy processing of polymers with the hardness of nanoparticles, functional hybrids can also incorporate other features by using the versatility of the solid substrate to carry catalysts, dyes, and drugs. Thus, they have a wide range of applications in hydrophobic, anticorrosion, conductive, antireflective, and photoactive materials. The utilization of polymer-coated silica nanoparticles can reduce particle aggregation in the films and achieve more homogeneous distribution of the inorganic components, resulting in better physicochemical properties.

Guo et al. synthesized a series of block-type amphiphilic copolymers via copolymerization of methacrylate end-capped oligo-urethane and MPS via the sol–gel process [167]. After hydrolysis and condensation of the copolymer precursors (self-assembled in the form of spherical micelles), polyurethane–silica hybrid materials with excellent thermal stability and mechanical properties were obtained. Etmimi et al. synthesized PS–GO nanocomposites via surface RAFT-mediated miniemulsion polymerization [155]. The molar mass and dispersity of PS in the nanocomposites were dependent on the amount of RAFT-grafted GO in the system. The PS–GO nanocomposites were of exfoliated morphology, and their thermal stability and mechanical properties were dependent on the modified GO content and better than those of neat PS polymer. Salami-Kalajahi et al. studied the effect of pristine nanoparticle loading on the properties of PMMA–silica nanocomposites prepared

via RAFT polymerization and found that the introduction of modified nanoparticles could result in better thermal and mechanical properties than those of pristine nanoparticles [168]. Surface modification and an increasing content of silica nanoparticles resulted in changes in the thermal degradation behavior of the nanocomposites. The best improvement in mechanical and thermophysical properties was achieved for nanocomposites containing 7 wt% silica nanoparticles. More recently, mechanically reinforced polymer–silica aerogels with PS and PBA segments were prepared by SI-RAFT, whereby well-defined polymers were grown on the silica surface to improve the mechanical strength compared with that of native aerogels [60]. The aerogel composites exhibited a low density of 0.13–0.17 g/cm^3, high thermal insulation performance of 0.03–0.04 W/(m · K), and a high specific surface area of 350–780 m^2/g, with approximately one order of magnitude improvement in the compression strength compared with the nonreinforced aerogels.

4.2 Bioactive Surfaces and Biomaterials

Polymer-grafted solid substrates with biocompatible or antibacterial polymers bound onto the surface can act as promising bioactive materials. Zhu et al. reported the preparation and properties of polyethersulfone (PES) ultrafiltration membranes with PHEMA-grafted silica nanoparticles as the blending additive [169]. Organic–inorganic hybrid membranes of PES with hybrid nanoparticles were fabricated via the traditional nonsolvent-induced phase separation (NIPS) process. The membrane surface porosity was increased and the surface hydrophilicity was enhanced after modification. Furthermore, the water permeability, solute rejection, and antifouling ability of PES membranes were also improved significantly. In contrast to traditional neat inorganic nanoparticle additives, the organic–inorganic hybrids could be held in/on PES membranes for a long period of time as a result of the intertwisting of polymer chains. Zhu et al. developed antifouling and antibacterial PES membranes by the addition of PDMAEMA-grafted silica nanoparticles and further postquaternization [170]. PES/SiO_2-*g*-PDMAEMA hybrid ultrafiltration membranes were prepared from the blending solutions via the NIPS process. The PDMAEMA chains incorporated into the PES membranes were further quaternized by reacting with 1,3-propane sultone and methyl iodide, respectively. The zwitterionic PES membranes exhibited excellent hydrophilicity, water permeability, solute rejection, and protein antifouling properties. The cationic membranes obtained from CH_3I treatment showed strong antibacterial activity against *E. coli* and *S. aureus* Rosenbach. Zhi et al. reported preparation of polyacrylonitrile (PAN)-based composite membranes by immersion precipitation using PDMAEMA-grafted silica nanoparticles as hydrophilic additive [171]. The synthesized nanoparticles had a typical core–shell structure, and the prepared PAN-based composite membranes had higher porosity and water permeation flux than the pure PAN membranes. As a result of the good hydrophilicity of the hybrid

nanoparticles, the membranes also showed high rejection (≥90%) of bovine serum albumin and high flux recovery ratio (≥90%) to water permeation.

Functional hybrid samples with tunable pores and stimuli-responsive grafts are promising as carriers for drug and gene delivery. A wide range of functional polymers such as PDMAEMA [172–174], PNIPAM [175], PAA [176], poly [2-(diethylamino)ethyl methacrylate]-*b*-poly[oligo(ethylene glycol) methacrylate] [177], and PAA-*b*-poly[poly(ethylene glycol) acrylate] [178] have been successfully grafted onto solid substrates for drug and gene delivery applications. The introduction of functional dyes and fluorescent molecules also allows hybrid materials to be used for therapeutic and diagnostic imaging applications[179–182].

4.3 Stationary Phases for Chromatographic Applications

Polymer-grafted silica has been widely utilized as a stationary phase in high performance liquid chromatography and shows satisfactory separation efficiency. These materials exhibit unique advantages such as high stability in extreme pH environments and sufficient retention for a variety of chemicals. As a result of heterogeneous structures and high mass-transfer resistance, polymer-grafted stationary phases normally exhibit lower column efficiency than traditional octadecyl-bonded silica. Controlled radical polymerization offers an efficient route to address this limitation as a result of its ability to provide more homogeneous structures and evenly distributed thin polymeric layers [183, 184]. PNIPAM-grafted silica can provide a thermoresponsive stationary phase in chromatography, and thus the separation can be adjusted by changing the temperature instead of changing the composition of the mobile phase [185, 186]. In addition to preparing a PS-bound chromatographic stationary phase [187, 188], Ali et al. also immobilized styrene-acrylamide copolymer on porous partially sub-2 μm silica monolith particles and the inner surface of fused silica capillary tubes (50 μm internal diameter and 28 cm length) to result in stationary phases for micro liquid chromatography (μLC) and capillary electrochromatography (CEC), respectively, for the separation of anomeric D-glucose derivatives [189]. RAFT polymerization was used to induce surface polymerization, and acrylamide was employed to incorporate amide functionality in the stationary phase. The resultant stationary phases were able to separate isomers of D-glucose derivatives with high selectivity and efficiency. The CEC stationary phase also gave good separation of other saccharides such as maltotriose and Dextran 1500 (molecular weight of about 1,500) with good separation efficiency (number of theoretical plates was about 300,000/m). Zhang and coworkers developed a tandem RAFT/click chemistry method for preparation of amide-polystyrene-silica (NHCO-PS-silica) stationary phase [190]. Styrene was immobilized on the amino-silica surface via an azide-functionalized RAFT agent in a one-pot procedure. The resultant NHCO-PS-silica column demonstrated better performance for shielding of residue silanols than traditional octadecylsilyl

columns, which was ascertained by Engelhardt, Tanaka, Galushko, and Walters tests. The NHCO-PS-silica was suitable for the separation of basic compounds, and this column also showed excellent stability with pure water as mobile phase.

4.4 Preparation of Hollow Capsules

Some methods such as layer-by-layer self-assembly [191], distillation precipitation polymerization [192–199], and surface-initiated polymerization [61, 200–202] have been developed for preparation of functional core–shell hybrids and composites. Using polymer-grafted solid substrates as precursors, functional hollow objects with multipurpose applications can be obtained by chemical postmodification such as etching and dissolving to remove the cores. Huang et al. reported controlled synthesis of photocrosslinked polymeric nanocapsules by SI-RAFT [61]. Narrowly distributed hollow polymeric nanocapsules (P*t*BMA-*co*-PDMIPM-*b*-PHPMA) of 450 or 900 nm diameter were prepared by exploiting silica nanoparticles as sacrificial templates and 2,3-dimethylmaleic imidopropyl methacrylate (DMIPM) as a photocrosslinker. A wall thickness of 10 nm could be achieved by using grafted block copolymer with molecular weight of 19,500 g/mol. Rahman and Elaissari developed a versatile method employing emulsion polymerization and precipitation polymerization to prepare rigid submicron-sized hollow capsules with a temperature-responsive shell [201]. After dissolving the inner magnetic core, PDVB@P(NIPAM-*co*-AEMA) hollow microcapsules with submicron size, narrow size distribution, cationic surface charge, and volume phase transition above the lower critical solution temperature (LCST) of the shell were obtained. The volume phase transition behavior of the outer shell layer can be utilized as an on/off switch to control the permeability of biomolecules or drugs into/out of the hollow capsules. Panahian reported the synthesis of dual thermo- and pH-sensitive hollow nanospheres based on poly(AA-*b*-HEMA) using an atom transfer reversible addition–fragmentation radical process [202]. A surface-attached ATRP initiator was converted to a RAFT agent, and acrylic acid and HEMA were polymerized via grafting-from RAFT polymerization. The PAA block was partially crosslinked via an esterification reaction, and hollow nanospheres were obtained by etching the silica cores with aqueous hydrofuran solution. These hollow nanospheres exhibited dual pH-sensitive and thermosensitive properties. One LCST of the particles was noted at low contents, whereas two LCSTs were observed at higher contents.

4.5 Molecularly Imprinted Polymer Films

Molecularly imprinted polymer (MIP) films are tailor-made synthetic polymers with a predetermined selectivity for a given analyte or group of structurally related

compounds, and they are usually obtained by polymerization in the presence of molecular templates [203]. MIPs contain binding sites for target molecules, with affinities and specificities on a par with those of natural receptors involving antibodies, hormone receptors, and enzymes. Thus, they can act as ideal materials for applications in areas such as CEC [204], detection of low molecular mass analytes [205], inducing protein crystallization [206], ion recognition [207], electro-analysis [208], solid-phase micro-extraction [209], and chemical sensors [210–213]. Recent advances in MIPs films prepared via RAFT-based techniques are listed below.

Titirici and Sellergren reported MIP thin films in which mesoporous silica beads modified with an azo initiator were used for grafting of crosslinked MIPs via a RAFT process [214]. Graft copolymerization of methacrylic acid and ethylene glycol dimethacrylate (EGDMA) mediated by 2-phenylprop-2-yl-dithiobenzoate in the presence of L-phenylalanine anilide as the template led to imprinted thin film composite beads. The resulting materials proved to be highly selective chiral stationary phases, resulting in baseline separation of the template racemate and structurally analogous racemates within a few minutes. These results were comparable with those obtained for materials prepared in the absence of RAFT mediation, with a notable difference being the absence of detectable solution gelation using RAFT. Lu et al. presented a general protocol for preparation of surface-imprinted core–shell nanoparticles via SI-RAFT [215]. The grafting copolymerization of 4-vinylpyridine and EGDMA in the presence of 2,4-dichlorophenoxyacetic acid as the template led to the formation of the target nanoparticles. Their potential use as the recognition element in the competitive fluorescent binding assay for 2,4-dichlorophenoxyacetic acid was also demonstrated. Li et al. reported preparation of MIP-grafted silica gel particles via SI-RAFT. The grafting copolymerization of methacrylic acid and divinyl benzene in the presence of template theophylline led to silica gel coated with a thin MIP film of about 1.98 nm thickness (MIP-silica) [216]. The measured binding kinetics for theophylline to the MIP-silica and for MIPs prepared by conventional bulk polymerization demonstrated that MIP-silica had improved mass-transfer properties. In addition, the theophylline-imprinted MIP-silica was used as the sorbent in solid-phase extraction to determine theophylline in blood serum, with satisfactory recovery higher than 90%. Nonspecific adsorption of interfering compounds could be eliminated by simple elution with acetonitrile, without sacrificing the selective binding of theophylline. Xu et al. developed an effective method for preparation of uniform surface-imprinted core–shell nanoparticles for determination of trace atrazine [217]. As a result of the advantages of controlled/living polymerization and surface-imprinting technology, the resultant RAFT surface-imprinted nanosized polymers (RAFT-SINPs) were spherically shaped particles with excellent monodispersity and demonstrated improved imprinting efficiency and mass transfer in comparison with MIPs prepared by traditional precipitation polymerization. Recoveries of 93.4% and 79.8% were achieved by one-step extraction when RAFT-SINPs were used for the pre-concentration and selective separation of atrazine in spiked corn and lettuce samples, respectively. These results enabled the separation and enrichment of

atrazine from complicated matrices using RAFT-SINPs. Halhalli et al. developed an improved grafting technique for production of thin film composite beads, whereby MIP films were grafted from porous silica using immobilized azoinitiators in the absence or presence of RAFT-mediated control or by controlled radical polymerization using immobilized iniferters (compounds that act as initiator, transfer agent, and terminator) [218]. Composites prepared by exhaustive polymerization under dilute conditions using high RAFT/initiator ratios displayed strongly enhanced chromatographic performance in terms of retentivity and enantioselectivity. Halhalli et al. developed a two-step route to address the classical deficiencies of MIPs, such as low binding capacity and nonuniform binding sites [219]. The thin-walled beads were produced in two steps by first grafting thin MIP films from porous silica beads under controlled (RAFT) or noncontrolled conditions, and then removing the silica supports from the composites by etching. This method led to beads with nanometer-thin walls with structure, morphology, and recognition properties that strongly depended on the grafting chemistry (RAFT or non-RAFT), monomer dilution, and film thickness of the original composite. The beads prepared under RAFT control showed a further enhanced saturation capacity, significantly exceeding that of the reference material. The reduced hydrophobic character of the thin-walled materials indicated the existence of two separate pore systems with different pore wettabilities.

5 Conclusions and Outlook

The high versatility of RAFT polymerization has made it a method of choice for surface modification. The latest advances in surface-initiated polymerization have enabled synthesis of target hybrids and (nano)composites with well-controlled molecular weight and topology, relatively low polydispersity, and tunable structural parameters such as grafting density, hydrophobic/hydrophilic ratio, and thickness of polymeric shell. With the introduction of functional polymers, the resultant hybrid/composite samples have found multipurpose applications in various fields, including bioscience and nanotechnology, and they hold great promise for smart surface and interface materials.

In our opinion, the following three aspects will attract increasing attention in both polymer and material sciences in the near future. First, the utilization of facile and controlled synthetic methods, especially tandem or one-pot approaches, holds great promise in advanced synthesis of target hybrids for materials science and engineering because of their simplicity in terms of process and because they favor large-scale production. Second, the introduction of smart moieties and cleavable linkages into grafted chains imparts increasing functionality and application, a hot topic in next-generation hybrid materials. Third, solid substrates grafted with complex macromolecular architectures with tunable compositions and molecular parameters will be an enduring topic in polymer science, materials science, and the biosciences. Design and synthesis of novel topological polymers not only allows

rapid construction of functional hybrids and composites but also promotes progress in related disciplines such as physics, materials science, and biotechnology. Solid substrates grafted with more complex topological polymers such as V-shaped, hyperbranched, cyclic, comb-on-comb, miktobrush, and miktoarm star copolymers will attract increasing attention as the role of polymeric graft architecture on the relation between structure, property, and application is established.

Acknowledgment Y.Z. acknowledges the financial support from the National Natural Science Foundation of China (Grants 20844001, 20874067 and 21074081) and the Project Funded by the Priority Academic Program Development of Jiangsu Higher Education Institutions. S.P. acknowledges the Royal Society Wolfson Merit Award (WM130055) and the Monash-Warwick Alliance for financial support.

References

1. Moad G, Rizzardo E, Thang SH (2012) Aust J Chem 65(8):985–1076
2. Perrier S, Takolpuckdee P (2005) J Polym Sci A Polym Chem 43(22):5347–5393
3. Chiefari J, Chong YK, Ercole F, Krstina J, Jeffery J, Le TPT, Mayadunne RTA, Meijs GF, Moad CL, Moad G, Rizzardo E, Thang SH (1998) Macromolecules 31(16):5559–5562
4. Corpart P, Charmot D, Biadatti T, Zard SZ, Michelet D (1998) Patent application WO 9858974
5. Gody G, Maschmeyer T, Zetterlund PB, Perrier S (2013) Nat Commun 4:2505 doi: 10.1038/ncomms3505
6. Gody G, Maschmeyer T, Zetterlund PB, Perrier S (2014) Macromolecules 47(2):639–649
7. Gody G, Maschmeyer T, Zetterlund PB, Perrier S (2014) Macromolecules 47(10):3451–3460
8. Zetterlund PB, Gody G, Perrier S (2014) Macromol Theory Simul 23(5):331–339
9. Moad G, Rizzardo E, Thang SH (2005) Aust J Chem 58(6):379–410
10. Tsujii Y, Ejaz M, Sato K, Goto A, Fukuda T (2001) Macromolecules 34(26):8872–8878
11. Li CZ, Benicewicz BC (2005) Macromolecules 38(14):5929–5936
12. Li C, Han J, Ryu CY, Benicewicz BC (2006) Macromolecules 39(9):3175–3183
13. Ohno K, Ma Y, Huang Y, Mori C, Yahata Y, Tsujii Y, Maschmeyer T, Moraes J, Perrier S (2011) Macromolecules 44:8944–8953
14. Cash BM, Wang L, Benicewicz BC (2012) J Polym Sci A Polym Chem 50(13):2533–2540
15. Perrier S, Takolpuckdee P, Mars CA (2005) Macromolecules 38(16):6770–6774
16. Zhao YL, Perrier S (2006) Macromolecules 39(25):8603–8608
17. Zhao YL, Perrier S (2007) Macromolecules 40(25):9116–9124
18. Zhao YL, Perrier S (2007) Macromol Symp 248(1):94–103
19. Nguyen DH, Wood MR, Zhao YL, Perrier S, Vana P (2008) Macromolecules 41(19):7071–7078
20. Zhao GD, Zhang PP, Zhang CB, Zhao YL (2012) Polym Chem 3(7):1803–1812
21. Ranjan R, Brittain WJ (2007) Macromol Rapid Commun 28(21):2084–2089
22. Ranjan R, Brittain WJ (2007) Macromolecules 40(17):6217–6223
23. Ranjan R, Brittain WJ (2008) Macromol Rapid Commun 29(12-13):1104–1110
24. Rotzoll R, Vana P (2008) J Polym Sci A Polym Chem 46(23):7656–7666
25. Rotzoll R, Nguyen DH, Vana P (2009) Macromol Symp 275–276(1):1–12
26. Zhu MQ, Wang LQ, Exarhos GJ, Li ADQ (2004) J Am Chem Soc 126(9):2656–2657
27. Liu FY, Agarwal S (2015) Macromol Chem Phys 216(4):460–465
28. Williams PE, Jones ST, Walsh Z, Appel EA, Abo-Hamed EK, Scherman OA (2015) ACS Macro Lett 4(2):255–259

29. Oschmann B, Tahir MN, Mueller F, Bresser D, Lieberwirth I, Tremel W, Passerini S, Zentel R (2015) Macromol Rapid Commun. doi:10.1002/marc.201400647
30. Ebara M, Hoffman JM, Hoffman AS, Stayton PS, Lai JJ (2013) Langmuir 29(18):5388–5393
31. Kaupp M, Tischer T, Hirschbiel AF, Vogt AP, Geckle U, Trouillet V, Hofe T, Stenzel MH, Barner-Kowollik C (2013) Macromolecules 46(17):6858–6872
32. Kaupp M, Quick AS, Rodriguez-Emmenegger C, Welle A, Trouillet V, Pop-Georgievski O, Wegener M, Barner-Kowollik C (2014) Adv Funct Mater 24(36):5649–5661
33. Kos T, Anžlovar A, Pahovnik D, Žagar E, Orel ZC, Žigon M (2013) Macromolecules 46(17): 6942–6948
34. Ning Y, Fielding LA, Andrews TS, Growney DJ, Armes SP (2015) Nanoscale 7:6691–6702
35. Hu JM, Wu T, Zhang GY, Liu SY (2012) J Am Chem Soc 134(18):7624–7627
36. Baum M, Brittain WJ (2002) Macromolecules 35(3):610–615
37. Rotzoll R, Vana P (2009) Aust J Chem 62(11):1473–1478
38. Le-Masurier SP, Gody G, Perrier S, Granville AM (2014) Polym Chem 5(8):2816–2823
39. Gody G, Rossner C, Moraes J, Vana P, Maschmeyer T, Perrier S (2012) J Am Chem Soc 134(30):12596–12603
40. Santoyo-Gonzalez F, Hernandez-Mateo F (2009) Chem Soc Rev 38(12):3449–3462
41. de Soler-Illia GJ, Sanchez C, Lebeau B, Patarin J (2002) Chem Rev 102(11):4093–4138
42. Kickelbick G (2003) Prog Polym Sci 28(1):83–114
43. Radhakrishnan B, Ranjan R, Brittain WJ (2006) Soft Mater 2(5):386–396
44. Tsujii Y, Ohno K, Yamamoto S, Goto A, Fukuda T (2006) Adv Polym Sci 197:1–45
45. Barbey R, Lavanant L, Paripovic D, Schüwer N, Sugnaux C, Tugulu S, Klok HA (2009) Chem Rev 109(11):5437–5527
46. Guo TY, Liu P, Zhu JW, Song MD, Zhang BH (2006) Biomacromolecules 7(4):1196–1202
47. Chinthamanipeta PS, Kobukata S, Nakata H, Shipp DA (2008) Polymer 49(26):5636–5642
48. Yang YK, Yang ZF, Zhao Q, Cheng XJ, Tjong SC, Li RKY, Wan XT, Xie XL (2009) J Polym Sci A Polym Chem 47(2):467–484
49. Sobani M, Haddadi-Asl V, Salami-Kalajahi M, Roghani-Mamaqani H, Mirshafiei-Langari SA, Khezri K (2013) J Solgel Sci Technol 66(2):337–344
50. Stenzel MH, Zhang L, Huck WTS (2006) Macromol Rapid Commun 27(14):1121–1126
51. Hou TT, Zhang PP, Zhou XD, Cao XQ, Zhao YL (2010) Chem Commun 46(39):7397–7399
52. Nguyen DH, Vana P (2006) Polym Adv Technol 17(9-10):625–633
53. Huebner D, Koch V, Ebeling B, Mechau J, Steinhoff JE, Vana P (2015) J Polym Sci A Polym Chem 53(1):103–113
54. Wang L, Benicewicz BC (2013) ACS Macro Lett 2(2):173–176
55. Liu CH, Pan CY (2007) Polymer 48(13):3679–3685
56. Liu CH, Pan CY (2008) Chem J Chin Univ 29(2):404–408
57. Liu JL, Zhang LF, Shi SP, Chen SA, Zhou NC, Zhang ZB, Cheng ZP, Zhu XL (2010) Langmuir 26(18):14806–14813
58. Moraes J, Ohno K, Gody G, Maschmeyer T, Perrier S (2013) Beilstein J Org Chem 9: 1226–1234
59. Choi J, Schattling P, Jochum FD, Pyun J, Char K, Theato P (2012) J Polym Sci A Polym Chem 50(19):4010–4018
60. Maleki H, Duraes L, Portugal A (2015) J Mater Chem A 3(4):1594–1600
61. Huang X, Appelhans D, Formanek P, Simon F, Voit B (2011) Macromolecules 44(21): 8351–8360
62. Huang YK, Liu Q, Zhou XD, Perrier S, Zhao YL (2009) Macromolecules 42(15):5509–5517
63. Guo YF, Liu HH, Tang DD, Li CX, Zhao YL (2015) Polym Chem 6:2647–2658
64. Kolb HC, Finn MG, Sharpless KB (2001) Angew Chem Int Ed 40(11):2004–2021
65. Hein JE, Fokin VV (2010) Chem Soc Rev 39(4):1302–1315
66. Tunca U (2014) J Polym Sci A Polym Chem 52(22):3147–3165
67. Kade MJ, Burke DJ, Hawker CJ (2010) J Polym Sci A Polym Chem 48(4):743–750
68. Hoyle CE, Bowman CN (2010) Angew Chem Int Ed 49(9):1540–1573

69. Lowe AB (2014) Polym Chem 5(17):4820–4870
70. Hoyle CE, Lowe AB, Bowman CN (2010) Chem Soc Rev 39(4):1355–1387
71. Yang ZL, Xu XL, Zhao YX (2014) Prog Chem 26(6):996–1004
72. Chen JC, Liu MZ, Chen C, Gong HH, Gao CM (2011) ACS Appl Mater Interfaces 3(8): 3215–3223
73. Li Y, Benicewicz BC (2008) Macromolecules 41(21):7986–7992
74. Huang YK, Hou TT, Cao XQ, Perrier S, Zhao YL (2010) Polym Chem 1(10):1615–1623
75. Kotsuchibashi Y, Ebara M, Aoyagi T, Narain R (2012) Polym Chem 3(9):2545–2550
76. Chen KL, Zhao YH, Yuan XY (2014) Chem Res Chin Univ 30(2):339–342
77. Peng C, Pan W, Bao L, Chen S, Chen Y, Han MS, Xiong YQ, Xu WJ (2014) Polym Adv Technol 25(6):684–688
78. Han MS, Zhang XY, Li L, Peng C, Bao L, Ou EC, Xiaong YQ, Xu WJ (2014) Express Polym Lett 8(7):528–542
79. Hojjati B, Sui RH, Charpentier PA (2007) Polymer 48(20):5850–5858
80. Ngo VG, Bressy C, Leroux C, Margaillan A (2009) Polymer 50(14):3095–3102
81. Hojjati B, Charpentier PA (2010) Polymer 51(23):5345–5351
82. Crippa M, Bianchi A, Cristofori D, D'Arienzo M, Merletti F, Morazzoni F, Scotti R, Simonutti R (2013) J Mater Chem C 1(3):484–492
83. Viswanath A, Shen Y, Green AN, Tan R, Greytak AB, Benicewicz BC (2014) Macromolecules 47(23):8137–8144
84. Esteves ACC, Hodge P, Trindade T, Barros-Timmons AMMV (2009) J Polym Sci A Polym Chem 47(20):5367–5377
85. Liu WH, Greytak AB, Lee J, Wong CR, Park J, Marshall LF, Jiang W, Curtin PN, Ting AY, Nocera DG (2010) J Am Chem Soc 132(2):472–483
86. Das P, Claverie JP (2012) J Polym Sci A Polym Chem 50(14):2802–2808
87. Dilag J, Kobus H, Ellis AV (2013) Forensic Sci Int 228(1-3):105–114
88. Boyer C, Priyanto P, Davis TP, Pissuwan D, Bulmus V, Kavallaris M, Teoh WY, Amal R, Carroll M, Woodward R (2010) J Mater Chem 20(2):255–265
89. Li X, Bao MM, Weng YY, Yang K, Zhang WD, Chen GJ (2014) J Mater Chem B 2(34): 5569–5575
90. Sahoo B, Devi KSP, Banerjee R, Maiti TK, Pramanik P, Dhara D (2013) ACS Appl Mater Interfaces 5(9):3884–3893
91. Wang L, Cole M, Li JT, Zheng Y, Chen YP, Miller KP, Decho AW, Benicewicz BC (2015) Polym Chem 6(2):248–255
92. Sumerlin BS, Lowe AB, Stroud PA, Zhang P, Urban MW, McCormick CL (2003) Langmuir 19(14):5559–5562
93. Rossner C, Vana P (2014) Angew Chem Int Ed 53(46):12639–12642
94. Adokoh CK, Quan S, Hitt M, Darkwa J, Kumar P, Narain R (2014) Biomacromolecules 15(10):3802–3810
95. Ahmed M, Mamba S, Yang XH, Darkwa J, Kumar P, Narain R (2013) Bioconjug Chem 24(6):979–986
96. Parry AL, Clamson NA, Ellis J, Bernhard SSR, Davis BG, Cameron NR (2013) J Am Chem Soc 135(25):9362–9365
97. Jiang XZ, Housni A, Gody G, Boullanger P, Charreyre MT, Delair T, Narain R (2010) Bioconjug Chem 21(3):521–530
98. Kirkland-York S, Zhang YL, Smith AE, York AW, Huang FQ, McCormick CL (2010) Biomacromolecules 11(4):1052–1059
99. Duong HTT, Adnan NNM, Barraud N, Basuki JS, Kutty SK, Jung K, Kumar N, Davis TP, Boyer C (2014) J Mater Chem B 2(31):5003–5011
100. Boyer C, Bousquet A, Rondolo J, Whittaker MR, Stenzel MH, Davis TP (2010) Macromolecules 43(8):3775–3784
101. Takara M, Toyoshima M, Seto H, Hoshino Y, Miura Y (2014) Polym Chem 5(3):931–939
102. Lu JW, Zhang WD, Richards SJ, Gibson MI, Chen GJ (2014) Polym Chem 5(7):2326–2332

103. Boyer C, Whittaker MR, Chuah K, Liu JQ, Davis TP (2010) Langmuir 26(4):2721–2730
104. Boyer C, Whittaker MR, Luzon M, Davis TP (2009) Macromolecules 42(18):6917–6926
105. Boyer C, Whittaker MR, Nouvel C, Davis TP (2010) Macromolecules 43(4):1792–1799
106. Rossner C, Ebeling B, Vana P (2013) ACS Macro Lett 2(12):1073–1076
107. Zhang T, Wu YP, Pan XM, Zheng ZH, Ding XB, Peng YX (2009) Eur Polym J 45(6): 1625–1633
108. Ebeling B, Vana P (2013) Macromolecules 46(12):4862–4871
109. Zhang T, Zheng ZH, Ding XB, Peng YX (2008) Macromol Rapid Commun 29(21): 1716–1720
110. Shan J, Nuopponen M, Jiang H, Kauppinen E, Tenhu H (2003) Macromolecules 36(12): 4526–4533
111. Beija M, Marty JD, Destarac M (2011) Chem Commun 47(10):2826–2828
112. Liu J, Detrembleur C, De Pauw-Gillet MC, Momet S, Duguet E, Jérôme C (2014) Polym Chem 5(3):799–813
113. Beija M, Palleau E, Sistach S, Zhao XG, Ressier L, Mingotaud C, Destarac M, Marty JD (2010) J Mater Chem 20(42):9433–9442
114. Gibson MI, Danial M, Klok HA (2011) ACS Comb Sci 13(3):286–297
115. Luo SZ, Xu J, Zhang YF, Liu SY, Wu C (2005) J Phys Chem B 109(47):22159–22166
116. Hotchkiss JW, Lowe AB, Boyes SG (2007) Chem Mater 19(1):6–13
117. Zhuang YY, Zhu Q, Tu CL, Wang DL, Wu JL, Xia YM, Tong GS, He L, Zhu BS, Yan DY (2012) J Mater Chem 22(45):23852–23860
118. Roy D, Semsarilar M, Guthrie JT, Perrier S (2009) Chem Soc Rev 38(7):2046–2064
119. Eichhorn SJ (2011) Soft Mater 7(2):303–315
120. Malmstrom E, Carlmark A (2012) Polym Chem 3(7):1702–1713
121. Carlmark A (2013) Macromol Chem Phys 214(14):1539–1544
122. Carlsson L, Fall A, Chaduc I, Wagberg L, Charleux B, Malmstrom E, D'Agosto F, Lansalot M, Carlmark A (2014) Polym Chem 5(20):6076–6086
123. Barsbay M, Guven G, Stenzel MH, Davis TP, Barner-Kowollik C, Barner L (2007) Macromolecules 40(20):7140–7147
124. Barsbay M, Kodama M, Guven O (2014) Cellulose 21(6):4067–4079
125. Goldmann AS, Tischer T, Barner L, Bruns M, Barner-Kowollik C (2011) Biomacromolecules 12(4):1137–1145
126. Demirci S, Celebioglu A, Uyar T (2014) Carbohydr Polym 113:200–207
127. Roy D, Knapp JS, Guthrie JT, Perrier S (2008) Biomacromolecules 9(1):91–99
128. Roy D, Guthrie JT, Perrier S (2008) Soft Mater 4(1):145–155
129. Roy D, Guthrie JT, Perrier S (2006) Aust J Chem 59(10):737–741
130. Xiao C, Xia C (2013) Int J Biol Macromol 52:349–352
131. Yuan J, Huang XB, Li PF, Li L, Shen J (2013) Polym Chem 4(19):5074–5085
132. Roy D, Guthrie JT, Perrier S (2005) Macromolecules 38(25):10363–10372
133. Barsbay M, Guven O, Davis TP, Barner-Kowollik C, Barner L (2009) Polymer 50(4): 973–982
134. Chen J, Yi J, Sun P, Liu ZT, Liu ZW (2009) Cellulose 16(6):1133–1145
135. Liu X, Chen J, Sun P, Liu ZW, Liu ZT (2010) React Funct Polym 70(12):972–979
136. Liu Y, Jin XS, Zhang XS, Han MM, Ji SX (2015) Carbohydr Polym 117:312–318
137. Kodama Y, Barsbay M, Guven O (2014) Radiat Phys Chem 94:98–104
138. Hiltunen M, Riihela S, Maunu SL (2009) J Polym Sci B Polym Phys 47(19):1869–1879
139. Hufendiek A, Trouillet V, Meier MAR, Barner-Kowollik C (2014) Biomacromolecules 15(7):2563–2572
140. Zeinali E, Haddadi-Asl V, Roghani-Mamaqani H (2014) RSC Adv 4(59):31428–31442
141. Novoselov K, Geim A, Morozov S, Jiang D, Zhang Y, Dubonos S, Grigorieva I, Firsov A (2004) Science 306(5696):666–669
142. Novoselov K, Geim A, Morozov S, Jiang D, Grigorieva M, Dubonos S, Firsov A (2005) Nature 438(7065):197–200

143. Stankovich S, Dikin D, Dommett G, Kohlhaas K, Zimney E, Stach E, Piner R, Nguyen S, Ruoff R (2006) Nature 442(7100):282–286
144. Dreyer DR, Park S, Bielawski CW, Ruoff RS (2010) Chem Soc Rev 39(1):228–240
145. Kim H, Abdala AA, Macosko CW (2010) Macromolecules 43(16):6515–6530
146. Badri A, Whittaker MR, Zetterlund PB (2012) J Polym Sci A Polym Chem 50(15): 2981–2992
147. Layek RK, Nandi AK (2013) Polymer 54(19):5087–5103
148. Thickett SC, Zetterlund PB (2013) Curr Org Chem 17(9):956–974
149. Li Y, Li X, Dogn CK, Qi JY, Han XJ (2010) Carbon 48(12):3427–3433
150. Layek RK, Kuila A, Chatterjee DP, Nandi AK (2013) J Mater Chem A 1(36):10863–10874
151. Ye YS, Chen YN, Wang JS, Rick J, Huang YJ, Chang FC, Hwang BJ (2012) Chem Mater 24(15):2987–2997
152. Peeters M, Kobben S, Jimenez-Monroy KL, Modesto L, Kraus M, Vandenryt T, Gaulke A, van Grinsven B, Ingebrandt S, Junkers T (2014) Sensor Actuat B Chem 203:527–535
153. Liu Y, Meng XG, Luo M, Meng MJ, Ni L, Qiu J, Hu ZY, Liu FF, Zhong GX, Liu ZC (2015) J Mater Chem A 3(3):1287–1297
154. Beckert F, Friedrich C, Thomann R, Mulhaupt R (2012) Macromolecules 45(17):7083–7090
155. Etmimi HM, Tonge MP, Sanderson RD (2011) J Polym Sci A Polym Chem 49(7):1621–1632
156. Gu RP, Xu WZ, Charpentier PA (2014) Polymer 55(21):5322–5331
157. Cui L, Liu JQ, Wang R, Liu Z, Yang WR (2012) J Polym Sci A Polym Chem 50(21): 4423–4432
158. Nikdel M, Salami-Kalajahi M, Hosseini MS (2014) RSC Adv 4(32):16743–16750
159. Gu R, Xu WZ, Charpentier PA (2013) J Polym Sci A Polym Chem 51(18):3941–3949
160. Liu ZZ, Lu GL, Li YJ, Li YS, Huang XY (2014) RSC Adv 4(105):60920–60928
161. Zhang B, Chen Y, Zhuang XD, Liu G, Yu B, Kang ET, Zhu JH, Li YX (2010) J Polym Sci A Polym Chem 48(12):2642–2649
162. Zhang B, Chen Y, Xu LQ, Zeng LJ, He Y, Kang ET, Zhang JJ (2011) J Polym Sci A Polym Chem 49(9):2043–2050
163. Zhang PP, Jiang K, Ye CN, Zhao YL (2011) Chem Commun 47(33):9504–9506
164. Jiang K, Ye CN, Zhang PP, Wang XS, Zhao YL (2012) Macromolecules 45(3):1346–1355
165. Nazir T, Afzal A, Siddiqi HM, Ahmad Z, Dumon M (2010) Prog Org Coat 69(1):100–106
166. Yan W, Han ZJ, Phung BT, Ostrikov KK (2012) ACS Appl Mater Interfaces 4(5):2637–2642
167. Guo SZ, Zhang C, Wang WZ, Liu TX (2010) Express Polym Lett 4(1):17–25
168. Salami-Kalajahi M, Haddadi-Asl V, Rahimi-Razin S, Behboodi-Sadabad F, Najafi M, Roghani-Mamaqani H (2012) J Polym Res 19(2):9793
169. Zhu LJ, Zhu LP, Jiang JH, Yi Z, Zhao YF, Zhu BK, Xu YY (2014) J Membr Sci 451:157–168
170. Zhu LJ, Zhu LP, Zhao YF, Zhu BK, Xu YY (2014) J Mater Chem A 2(37):15566–15574
171. Zhi SH, Deng R, Xu J, Wan LS, Xu ZK (2015) React Funct Polym 86:184–190
172. Zhang YF, Gu WY, Xu HX, Liu SY (2008) J Polym Sci A Polym Chem 46(7):2379–2389
173. Sun JT, Yu ZQ, Hong CY, Pan CY (2012) Macromol Rapid Commun 33(9):811–818
174. Majewski AP, Stahlschmidt U, Jerome V, Freitag R, Müller AHE, Schmalz H (2013) Biomacromolecules 14(9):3081–3090
175. Hong CY, Li X, Pan CY (2008) J Phys Chem C 112(39):15320–15324
176. Hong CY, Li X, Pan CY (2009) J Mater Chem 19(29):5155–5160
177. Zhou JM, Zhang WJ, Hong CY, Pan CY (2015) ACS Appl Mater Interfaces 7(6):3618–3625
178. Cui L, Wang R, Ji XQ, Hu M, Wang B, Liu JQ (2014) Mater Chem Phys 148(1-2):87–95
179. Müllner M, Schallon A, Walther A, Freitag R, Müller AHE (2010) Biomacromolecules 11(2):390–396
180. Wan XJ, Wang D, Liu SY (2010) Langmuir 26(19):15574–15579
181. Moraes J, Ohno K, Maschmeyer T, Perrier S (2013) Chem Mater 25(17):3522–3527
182. Ji WD, Li NJ, Chen DY, Qi XX, Sha WW, Jiao Y, Xu QF, Li JM (2013) J Mater Chem B 43(43):5942–5949
183. Hemstrom P, Szumski M, Irgum K (2006) Anal Chem 78(20):7098–7103

184. Ni CH, Wang WT, Zhu CP, Huang B, Yao BL (2010) Soft Mater 8(1):14–28
185. Roohi F, Titirici MM (2008) New J Chem 32(8):1409–1414
186. Roohi F, Antonietti M, Titirici MM (2008) J Chromatogr A 1203:160–167
187. Ali F, Cheong WJ, Alothman ZA, Almajid AM (2013) J Chromatogr A 1303:9–17
188. Ali F, Kim YS, Lee JW, Cheong WJ (2014) J Chromatogr A 1324:115–120
189. Ali F, Kim YS, Cheong WJ (2014) Bull Korean Chem Soc 35(2):539–545
190. Zhang Z, Chen ML, Cheng XD, Shi ZG, Yuan BF, Feng YQ (2014) J Chromatogr A 1351: 96–102
191. Yang XL, Zhu YH, Zhu MQ, Li CZ (2003) J Inorg Mater 18(6):1293–1298
192. Liu GY, Zhang H, Yang XL, Wang YM (2007) Polymer 48(20):5896–5904
193. Liu GY, Ji HF, Yang XL, Wang YM (2008) Langmuir 24(3):1019–1025
194. Liu GY, Yang XL, Wang YM (2008) Langmuir 24(10):5485–5491
195. Liu GY, Wang H, Yang XL (2009) Polymer 50(12):2578–2586
196. Zhang H, Yang XL (2010) Polym Chem 1(5):670–677
197. Ji M, Liu HL, Yang XL (2011) Polym Chem 2(1):148–156
198. Li GL, Xu LQ, Tang XZ, Neoh KG, Kang ET (2010) Macromolecules 43(13):5797–5803
199. Li GL, Wan D, Neoh KG, Kang ET (2010) Macromolecules 43(24):10275–10282
200. Wu T, Ge ZS, Liu SY (2011) Chem Mater 23(9):2370–2380
201. Rahman MM, Elaissari A (2012) J Mater Chem 22(3):1173–1179
202. Panahian P, Salami-Kalajahi M, Hosseini MS (2014) Ind Eng Chem Res 53(19):8079–8086
203. Bompart M, Haupt K (2009) Aust J Chem 62(8):751–761
204. Turiel E, Martin-Esteban A (2005) J Sep Sci 28(8):719–728
205. Uludag Y, Piletsky SA, Turner APF, Cooper MA (2007) FEBS J 274(21):5471–5480
206. Saridakis E, Chayen NE (2013) Trends Biotechnol 31(9):515–520
207. Wu XY (2012) Mikrochim Acta 176(1-2):23–47
208. Cervini P, Cavalheiro ETG (2012) Anal Lett 45(4):297–313
209. Zhang MS, Zeng JB, Wang YR, Chen X (2013) J Chromatogr Sci 51(7):577–586
210. Fuchs Y, Soppera O, Haupt K (2012) Anal Chim Acta 717:7–20
211. Lofgreen JE, Ozin GA (2014) Chem Soc Rev 43(3):911–933
212. Algieri C, Drioli E, Guzzo L, Donato L (2014) Sensors 14(8):13863–13912
213. Wackerlig J, Lieberzeit PA (2015) Sensor Actuat B Chem 207:144–157
214. Titirici MM, Sellergren B (2006) Chem Mater 18(7):1773–1779
215. Lu CH, Zhou WH, Han B, Yang HH, Chen X, Wang XR (2007) Anal Chem 79(14): 5457–5461
216. Li Y, Zhou WH, Yang HH, Wang XR (2009) Talanta 79(2):141–145
217. Xu SF, Li JH, Chen LX (2011) J Mater Chem 21(12):4346–4351
218. Halhalli MR, Aureliano CSA, Schillinger E, Sulitzky C, Titirici MM, Sellergren B (2012) Polym Chem 3(4):1033–1042
219. Halhalli MR, Schillinger E, Aureliano CSA, Sellergren B (2012) Chem Mater 24(15): 2909–2919